Electronic Supporting Information

Highly efficient oxidative cleavage of lignin β-O-4 linkages via synergistic Co-CoO_x/N-doped carbon and recyclable hexaniobate catalysis

Jie Li,[a] Pengpeng Shao,[a] Weijie Geng,[a] Peng Lei,[a] Jing Dong,[b] Yingnan Chi*[a] and Changwen Hu[a]

a Key Laboratory of Cluster Science Ministry of Education, Beijing Key Laboratory of Photoelectronic/Electrophotonic Conversion Materials, School of Chemistry and Chemical Engineering, Beijing Institute of Technology, Beijing 100081, P.R. China

b College of Chemistry and Materials Engineering, Beijing Technology and Business University, Beijing 100048, P.R. China

*Corresponding author (chiyingnan7887@bit.edu.cn)

Contents

Catalyst Characterization

Powder X-ray diffraction (PXRD) data were collected on a Rigaku MiniFlex 600 diffractometer with a Cu-Kα X-ray radiation source (λ = 1.54056 Å). Fourier-transform infrared (FT-IR) spectra were recorded at the range 4000-400 cm^{-1} on a Bruker ALPHA spectrometer. The Co content was measured by a ThermoiCAP Q mass spectrometry. The X-ray photoelectron spectroscopy (XPS) was conducted by the Thermo scientific Kα XPS equipped with a monochromatic Al Kα X-ray source (1486.6 eV). The morphologies of catalysts were observed on JEM-2010 transmission electron microscope. Electric paramagnetic resonance (EPR) signals were captured on a Bruker EMXplus. Two-dimensional Nuclear Magnetic Resonance Heteronuclear Single Quantum Coherence (2D NMR HSQC) spectra were recorded on a Bruker AVANCE III HD 700 MHz spectrometer. Gel permeation chromatography (GPC) was performed with a Waters 1515 chromatography system equipped with an Agilent PL1110 column. Gas chromatography-mass spectrometry (GC-MS) was used to identify substrate and products on an Agilent 7890A GC/5975C MS.

Preparation of Lignin β-O-4 Model Compounds

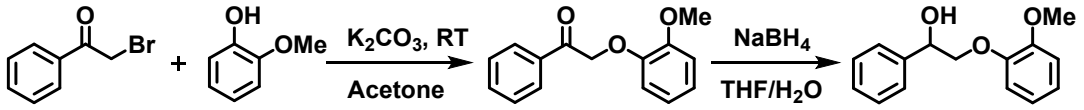

Synthesis of 2-(2-Methoxyphenoxy)-1-phenylethanol[1]: (i) To a solution of guaiacol (0.9 g, 7.3 mmol) in 15 mL acetone, K_2CO_3 (1.04 g, 7.5 mmol) was added and stirred for 30 min. Then, 2-bromoacetophenone (1.4 g, 7 mmol) was added. After reaction for 24 h, the filtrate was collected and concentrated by rotary evaporator in vacuum. The solid was added into EtOAc, washed with 5% NaOH solution and water. The organic phase was collected, dried over anhydrous Na_2SO_4 and evaporated in vacuum. The obtained powder was recrystallized in ethanol.

(ii) The above powder (0.212 g, 1 mmol) was dissolved completely into a mixed solution of THF/H_2O (4:1 volume ratio, 5 mL), and $NaBH_4$ (76 mg, 2 mmol) was added

and stirred at room temperature. After 1 h, excess saturated NH_4Cl aqueous solution (3 mL) was poured into the reaction mixture. Then, the liquid was extracted with EtOAc, washed with brine and dried over anhydrous Na_2SO_4. The organic phase was concentrated to obtain 2-(2-Methoxyphenoxy)-1-phenylethanol. Similarly, the synthetic steps of other methoxy group substituted 2-Phenoxy-1-phenylethanol were the same as that of 2-(2-Methoxyphenoxy)-1-phenylethanol, except that the starting materials were different.

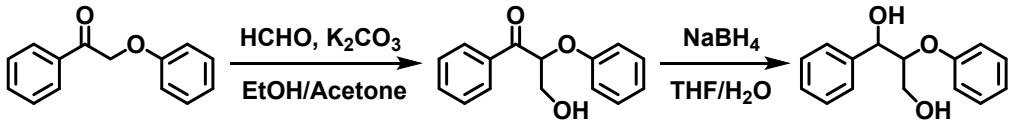

Synthesis of 2-phenoxy-1-phenylpropane-1,3-diol[1]: 2-phenoxyacetophenone was prepared by the above similar method. A mixed EtOH/acetone (1:1, 30 mL) solution containing 2-phenoxyacetophenone (1.27 g, 6.0 mmol), HCHO (36 wt%, 11 mmol) and K_2CO_3 (0.9 g, 6.5 mmol) was stirred for 4 h and evaporated. The residue was dissolved in EtOAc and washed with water and brine. The organic phase was concentrated and purified by column chromatography with petroleum ether/EtOAc. Then the ketone, 1-phenyl-3-hydroxy-2-phenoxy propan-1-one, was reduced with $NaBH_4$ in THF/H_2O to obtain diol.

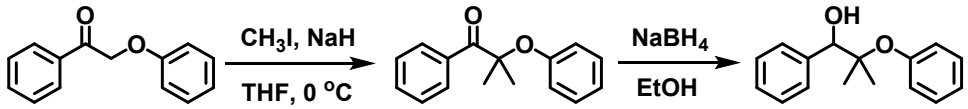

Synthesis of 2-methyl-2-phenoxy-1-phenylpropan-1-ol[2]: 2-phenoxyacetophenone (1.0 g, 4.8 mmol) was added to a three-neck bottle with anhydrous THF (26 mL). The bottle was placed in an ice bath, and in an Ar atmosphere NaH (0.64 g, 15.9 mmol, 60 wt% in mineral oil) was slowly added under stirring. After 15 min, CH_3I (0.99 g, 15.9 mmol) was dropped slowly. The mixture was heated at 40 °C for 4 h, followed by 30 mL of water and EtOAc. The extracted organic phase was washed with brine, dried over anhydrous Na_2SO_4, evaporated by rotary, and purified by column chromatography. Finally, 2-methyl-2-phenoxy-1-phenylpropan-1-ol was obtained by a similar reduction process in EtOH solvent.

Preparation of organosolv birch lignin[3]

A 500 mL round-bottom flask was charged with 1,4-dioxane (144 mL) and the dilute HCl (2 mol/L, 16 mL), and birch sawdust (20 g) was added. The mixture was heated to 80 ^{o}C under argon atmosphere for 1 h. The filtrate was collected and concentrated in vacuum. The grume was fully dissolved in acetone/water (9:1, 25 mL) and precipitated by the slowly addition into 250 mL of water. After being dried in air, the crude lignin was redissolved in acetone/methanol (9:1, 25 mL) and gradually added into Et_2O (200 mL) with a quick stir. The organosolv birch lignin was collected by filtration and dried in air, affording 1.47 g solid sample with a yield of 7.35%. Lignin purity was measured by national renewable energy laboratory (NREL) method with the acid insoluble lignin content of 73%. This exacted lignin was used in subsequent experiments without further processing.

Supplementary experimental results

Table S1. Different catalysts for the oxidative cleavage of β-O-4 alcohol under aerobic conditions.

entry	catalysts	base catalysts	reaction system	O_2	temp. (°C)	time (h)	conv. (%)	yield of phenols (%)	yield of benzoates (%)	ref.
1	(i) AcNH-TEMPO/ HCl/HNO_3 (ii) H_2O_2-NaOH	0.001 equiv. NaOH	Homo.	1 atm O_2 -	45 50	24 10	96 100	- 42	- -	[4]
2	AuPd-CTFs	-	Heter.	0.5 MPa	160	4	96	49	17	[1]
3	Pd/CeO_2	-	Heter.	0.1 MPa	185	24	64	48	14	[5]
4	Au/CeO_2	-	Heter.	1 MPa	180	4	72	45	31	[6]
5	RuMo/rGO	0.1 M NaOH	Heter.	0.3 MPa	100	12	94	49	-	[7]
6	VB_{12}/C-900	0.2 equiv. K_2CO_3	Heter.	0.1 MPa	80	24	96	96	73	[2]
7	Co-N-C	1 equiv. NaOH	Heter.	1 MPa air	150	4	93	69	86	[8]
8	Co@CN	-	Heter.	0.1 MPa	110	12	-	65	31	[9]
9	(i) $VOSO_4$/TEMPO (ii) $Cu(OAc)_2$/Phen	0.2 equiv. Phen	Homo.	0.4 MPa	100 80	12 3	82 94	- 85	- -	[10]
10	Bim-V-2	-	Homo.	0.5 MPa	120	10	97	92	32	[11]
11	(dipic)V(O)O^{i}Pr	-	Homo.	Air	100	168	95	77	-	[12]
12	$[Cu^I(bbi)]_2\{[Cu^I(bbi)]_2$-$V^{IV}_2V^V_8O_{26}\}\cdot 2H_2O$	-	Heter.	0.4 MPa	100	12	>99	60	90	[13]
13	$[MIMPS]_2H_4P_2Mo_{18}O_{62}$	-	Homo.	0.5 MPa	140	10	95	83.5	-	[14]
14	$H_5PMo_{10}V_2O_{40}$/$BMIMSO_3$	-	Homo.	1 atm O_2	130	10	100	80	-	[15]

15	$BetH_5V_2Mo_{18}O_{62}$	-	Homo.	0.8 MPa	140	8	92.9	86.3	1.8	[16]
16	$CoMA/C_{900}$-KNb_6	0.2 equiv. KNb_6	Heter.	0.2 MPa	100	3	99	99	98	This work

Heter. = Heterogeneous; Homo. = Homogeneous; temp. = temperature; conv. = conversion

Table S2. Different catalysts for the oxidative cleavage of β-O-4 ketone under aerobic conditions.

entry	catalysts	base catalysts	reaction system	O_2	temp. (°C)	time (h)	conv. (%)	yield of phenols (%)	yield of benzoates (%)	ref.
1	KNb_6-Cu/C_3N_4	0.058 equiv. KNb_6	Heter.	0.5 MPa	80	12	96	90	10	[17]
2	CTF-*p*DCB-1	-	Heter.	0.5 MPa	140	2	> 99	45	15	[18]
3	KO_x-CTFs	-	Heter.	0.5 MPa	120	2	62	52	8	[3]
4	$Cu(OAc)_2$	2 equiv. $BF_3{\cdot}OEt_2$	Homo.	0.4 MPa	90	2	86	39	51	[19]
5	CuCl	4 equiv. NaOH	Homo.	1 atm air	30	5.5	97	89	-	[20]
6	Ce-Cu/MFI	-	Heter.	1.0 MPa	150	24	100	-	41	[21]
7	Fe-N-C	-	Heter.	0.3 MPa	140	4	94	93	62	[22]
8	$CoMA/C_{900}$-KNb_6	0.2 equiv. KNb_6	Heter.	0.2 MPa	80	0.25	99	99	96	This work

Heter. = Heterogeneous; Homo. = Homogeneous; temp. = temperature; conv. = conversion

Table S3. Oxidative cleavage of PP-ol catalyzed by different catalysts. [a]

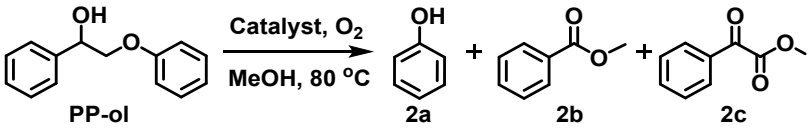

Entry	Catalyst	Temp. (°C)	Conv. (%)[b]	Yield (%)[b]		
				2a	**2b**	**2c**
1	Blank	80	<1	trace	trace	-
2	KNb_6	80	14	12	11	-
3	$CoMA/C_{900}$	80	37	36	24	11
4	$CoMA/C_{900}$-KNb_6	80	90	90	89	-
5	$CoMA/C_{900}$-KNb_6	40	30	30	27	-
6	$CoMA/C_{900}$-KNb_6	60	53	51	52	-
7	$CoMA/C_{900}$-KNb_6	100	99	99	98	-
8	$CoMA/C_{900}$-KNb_6	120	99	99	99	-
9	MA/C_{900}-KNb_6	80	16	16	15	1
10	$CoMA/C_{700}$-KNb_6	80	47	45	46	-
11	$CoMA/C_{800}$-KNb_6	80	57	56	41	13
12	$CoMA/C_{1000}$-KNb_6	80	74	73	66	-
13	Co powder-KNb_6	80	12	11	12	-
14	CoO-KNb_6	80	10	9	9	-
15	Co_3O_4-KNb_6	80	8	6	7	-
16	$CoMA/C_{900}$-350-KNb_6	80	11	8	10	-
17	$CoMA/C_{900}$-H^+-KNb_6	80	13	10	11	-

[a] Reaction conditions: PP-ol (0.05 mmol), $CoMA/C_{900}$-KNb_6 (40 mg, m : m = 5 : 3), 2.5 mL MeOH, 80 °C, 0.2 MPa O_2, t = 3 h, biphenyl as the internal standard. [b] Conversion and yield were monitored by GC with FID detector.

Table S4. Influence of KNb_6 amount and different bases on the cleavage of PP-one. [a]

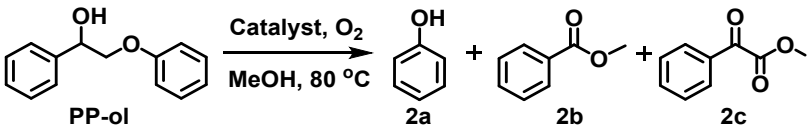

Entry	Catalyst	Conv. (%)[b]	Yield (%)[b]		
			2a	**2b**	**2c**
1	CoMA/C_{900}-KNb_6 (5:0)	37	36	24	11
2	CoMA/C_{900}-KNb_6 (5:1)	71	67	60	10
3	CoMA/C_{900}-KNb_6 (5:2)	86	86	75	11
4	CoMA/C_{900}-KNb_6 (5:3)	90	90	89	-
5	CoMA/C_{900}-KNb_6 (5:4)	93	86	92	-
6	CoMA/C_{900}-NaOH (0.2 eq.)	70	68	62	8
7	CoMA/C_{900}-KOH (0.2 eq.)	74	73	50	19
8	CoMA/C_{900}-K_2CO_3 (0.2 eq.)	70	70	59	7
9	CoMA/C_{900}-KOAc (0.2 eq.)	42	32	18	11
10	CoMA/C_{900}-Prydine (0.2 eq.)	36	35	28	8
11	CoMA/C_{900}-Et_3N (0.2 eq.)	48	45	24	21
12	CoMA/C_{900}-MgO (0.2 eq.)	41	33	25	12
13	CoMA/C_{900}-CaO (0.2 eq.)	62	57	48	10
14	CoMA/C_{900}-Nb_2O_5 (0.2 eq.)	40	39	27	10

[a] Reaction conditions: PP-ol (0.05 mmol), CoMA/C_{900} (25 mg), base (0.2 eq.), 2.5 mL MeOH, 80 °C, 0.2 MPa O_2, t = 3 h. [b] Conversion and yield were monitored by GC with FID detector.

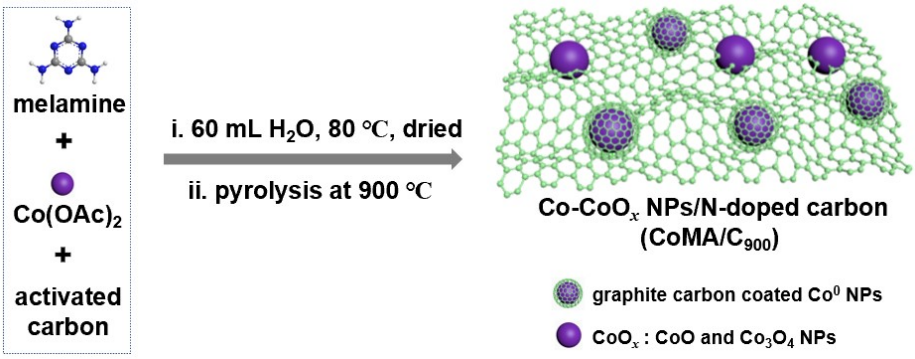

Scheme S1. The preparation of Co-CoO_x NPs/N-doped carbon.

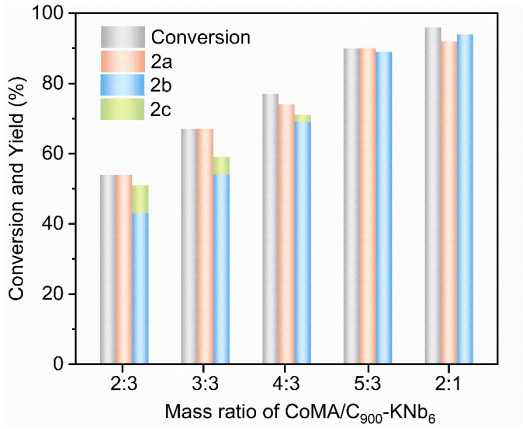

Figure S1. The optimization of reaction conditions by adjusting CoMA/C_{900} amount.

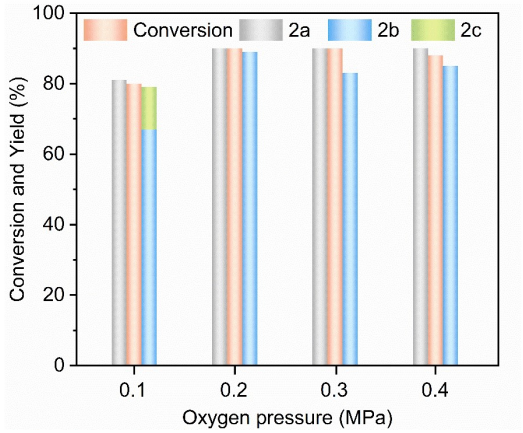

Figure S2. The optimization of reaction conditions by various oxygen pressure.

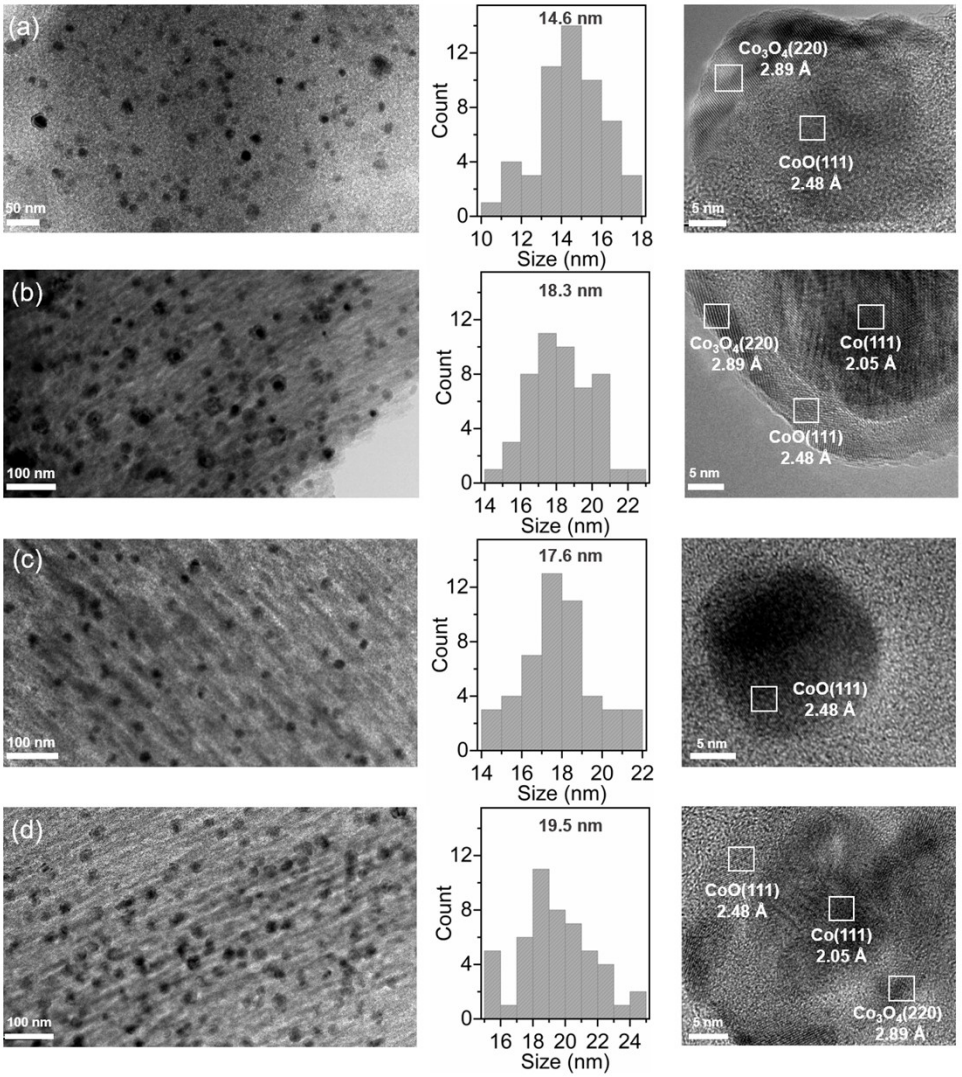

Figure S3. TEM image, the particle-size distribution histogram and HRTEM image of Co^0, CoO and/or Co_3O_4 NPs of (a) CoMA/C_{700}, (b) CoMA/C_{800}, (c) CoMA/C_{900}, (d) CoMA/C_{1000}.

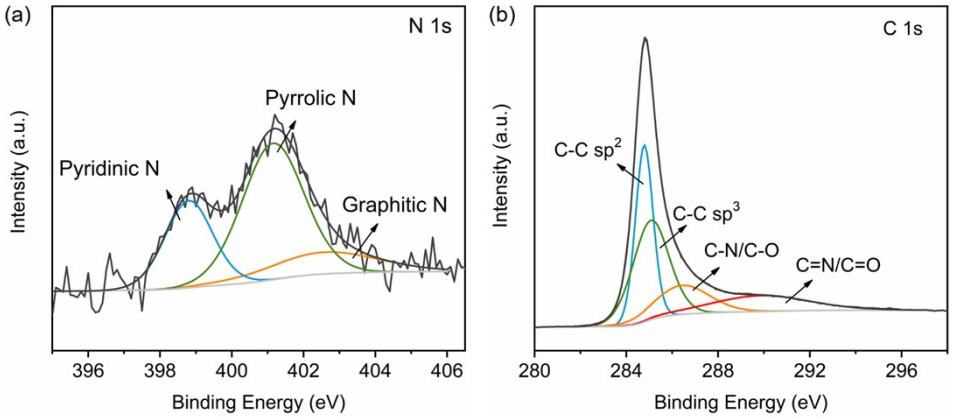

Figure S4. (a) N 1s and (b) C 1s XPS spectra of N-doped carbon support in CoMA/C_{900}.

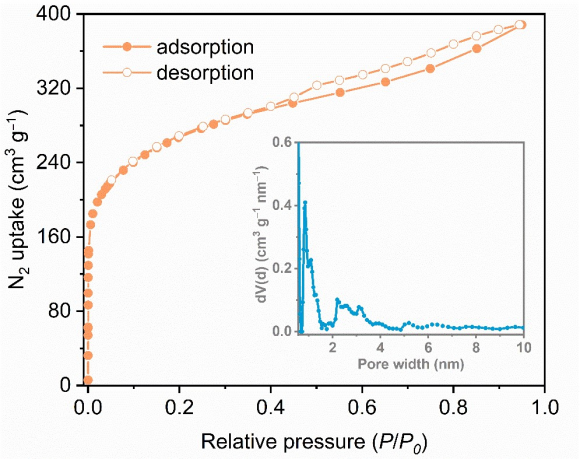

Figure S5. N_2 sorption isotherms of CoMA/C_{900}. Inset: Pore size distributions of CoMA/C_{900}.

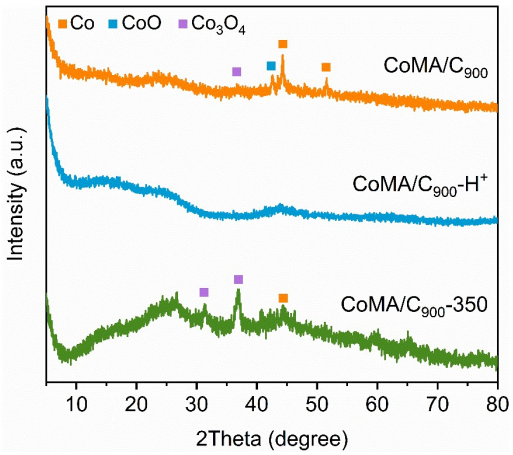

Figure S6. The PXRD patterns of CoMA/C_{900}, CoMA/C_{900}-H^+ and CoMA/C_{900}-350.

Table S5. Radical trapping experiments for the catalytic cleavage of PP-ol.[a]

Entry	Radical scavenger	Conv. (%)[b]	Yield (%)[b]	
			2a	**2b**
1	No	90	90	89
2[c]	No	< 1	< 1	< 1
3	Ph_2NH	20	20	16
4	BQ	3	3	3
5	BHT	20	20	16

[a] Reaction conditions: PP-ol (0.05 mmol), CoMA/C_{900}-KNb_6 (40 mg, m : m = 5 : 3), 2.5 mL MeOH, 80 °C, 0.2 MPa O_2, t = 3 h. [b] Conversion and yield were monitored by GC with FID detector. [c] 0.2 MPa N_2.

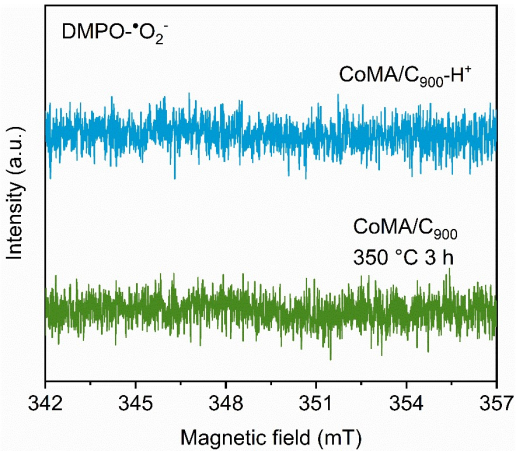

Figure S7. EPR patterns in the presence of CoMA/C_{900}-H^+ and CoMA/C_{900}-350 with DMPO as the trapping agent.

Table S6. The effect of solvent on the oxidative cleavage of PP-ol.[a]

Entry	solvent	Conv. (%)[b]	Yield (%)[b]	
			2a	**esters**
1	MeOH	90	90	89
2	EtOH	54	52	53
3	*i*-PrOH	37	36	31
4	*t*-BuOH	12	12	11
5	CH_3CN	9	5	-
6	THF	7	5	-
7	Diox	5	5	-

[a] Reaction conditions: PP-ol (0.05 mmol), CoMA/C_{900}-KNb_6 (40 mg, m : m = 5 : 3), 2.5 mL solvent, 80 °C, 0.2 MPa O_2, t = 3 h. [b] Conversion and yield were monitored by GC with FID detector.

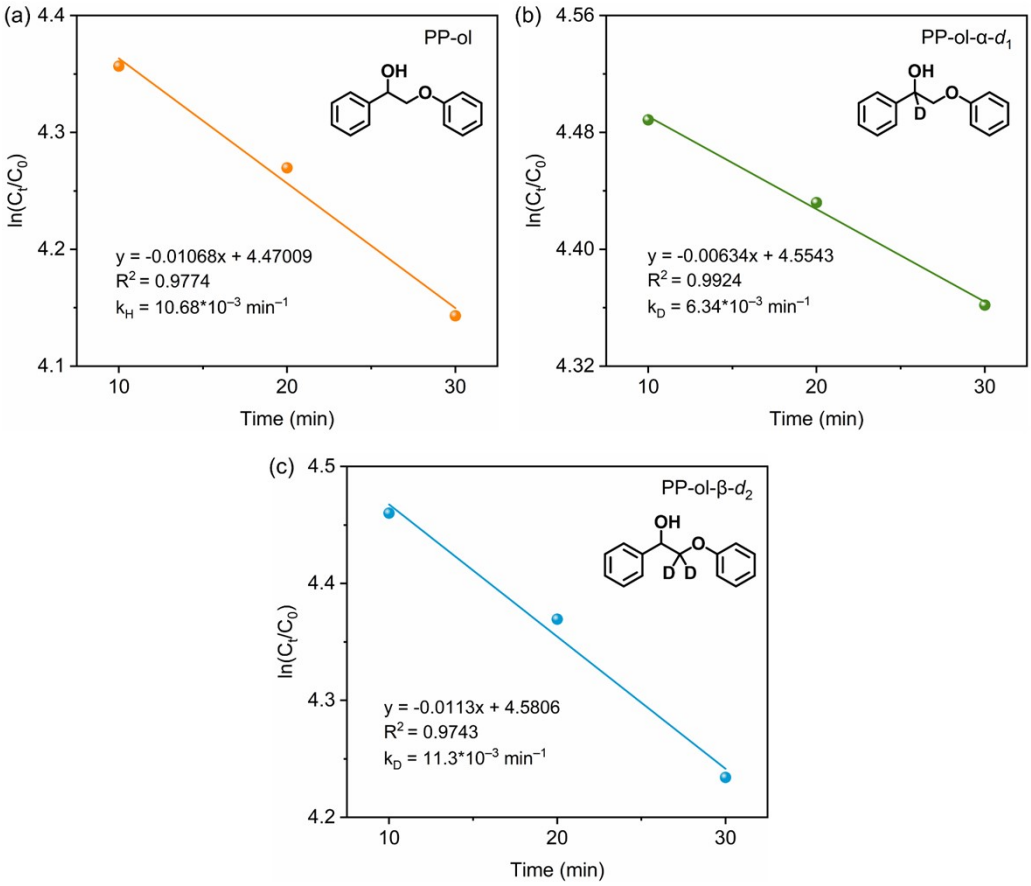

Figure S8. The linear fit of $\ln(C_t/C_0)$ against the reaction time (a) PP-ol and (b) PP-ol-α-d_1 and (c) PP-ol-β-d_2 catalyzed by CoMA/C_{900}-KNb_6.

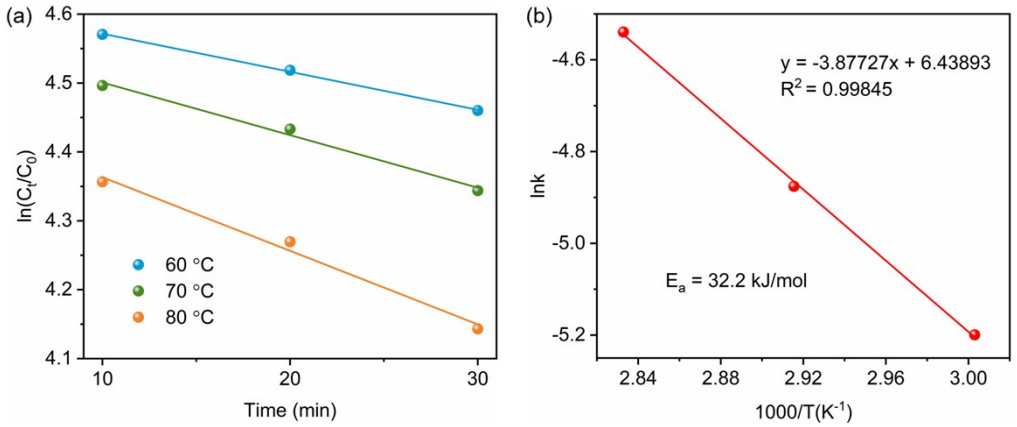

Figure S9. The measurement of apparent activation energy at 60, 70, and 80 °C. The data obtained fit to the first order kinetic.

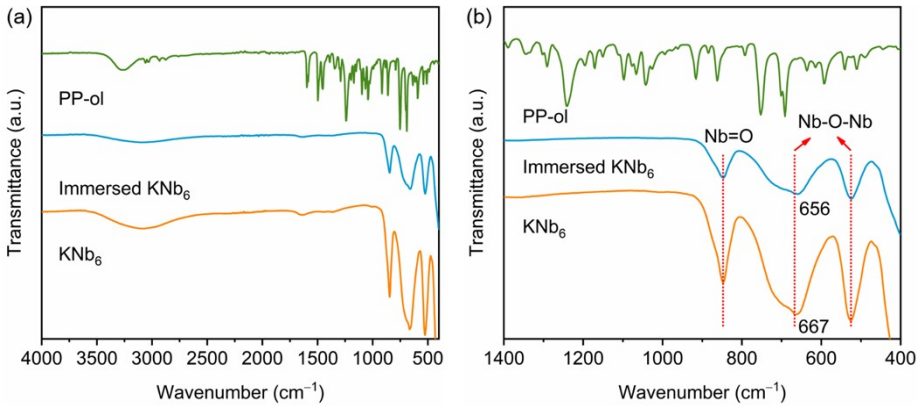

Figure S10. FT-IR spectra of PP-ol, fresh and immersed KNb_6 with the wavenumber range of (a) 4000-400 cm^{-1} and (b) 1400-400 cm^{-1}. KNb_6 was immersed in a minimal amount of methanol containing PP-ol, followed by separation, washing, and drying of the KNb_6.

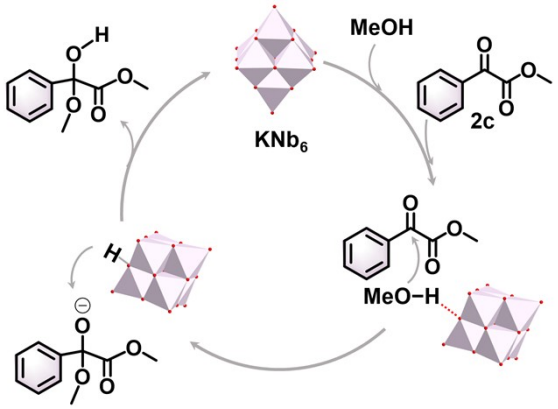

Figure S11. The possible role of KNb_6 during the process of MeOH attacking C_α site of methyl benzoylformate (**2c**).

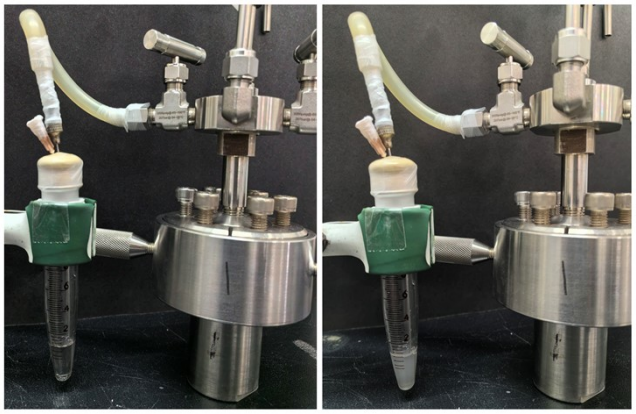

Figure S12. The detection of CO_2 produced during reaction through a clear limewater.

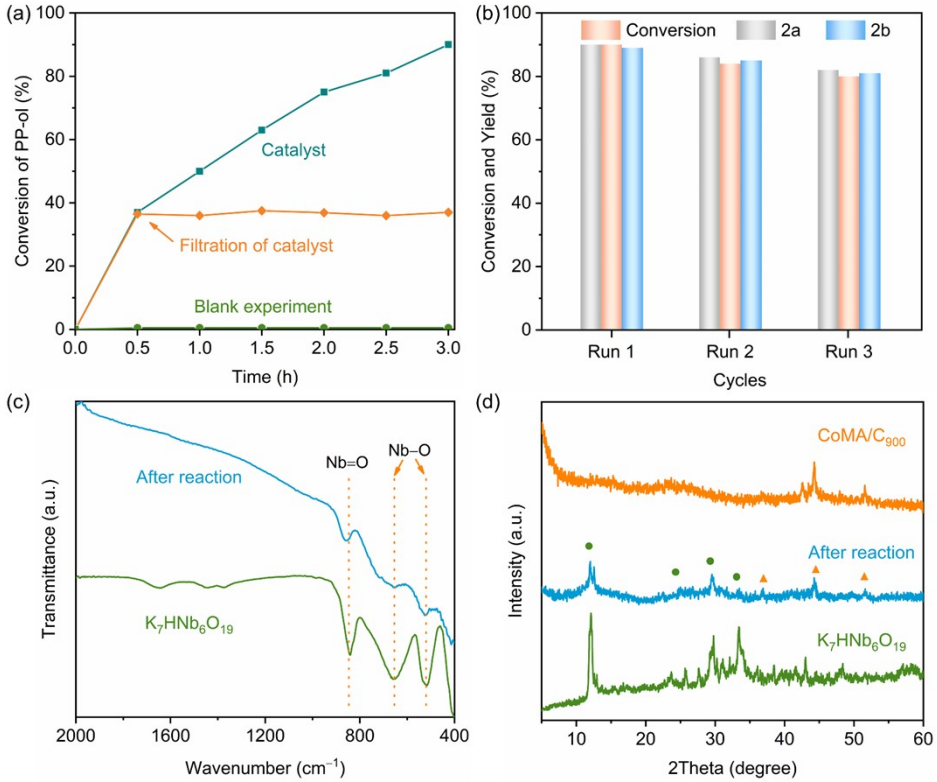

Figure S13. (a) Leaching test for the conversion of PP-ol to aromatic monomers over CoMA/C_{900}-KNb_6. (b) Recycling test. (c) FT-IR and (d) PXRD of the fresh and used catalysts.

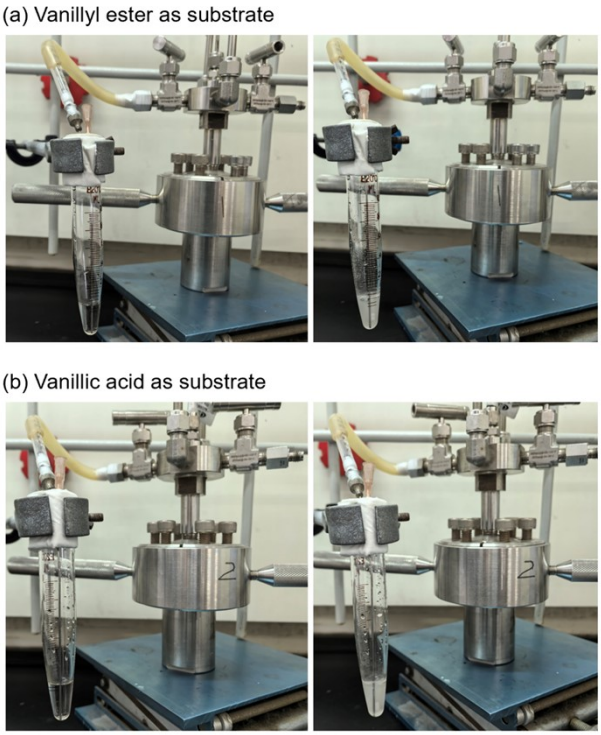

Figure S14. The detection of CO_2 by a clear limewater using vanillyl ester and vanillic acid as substrate.

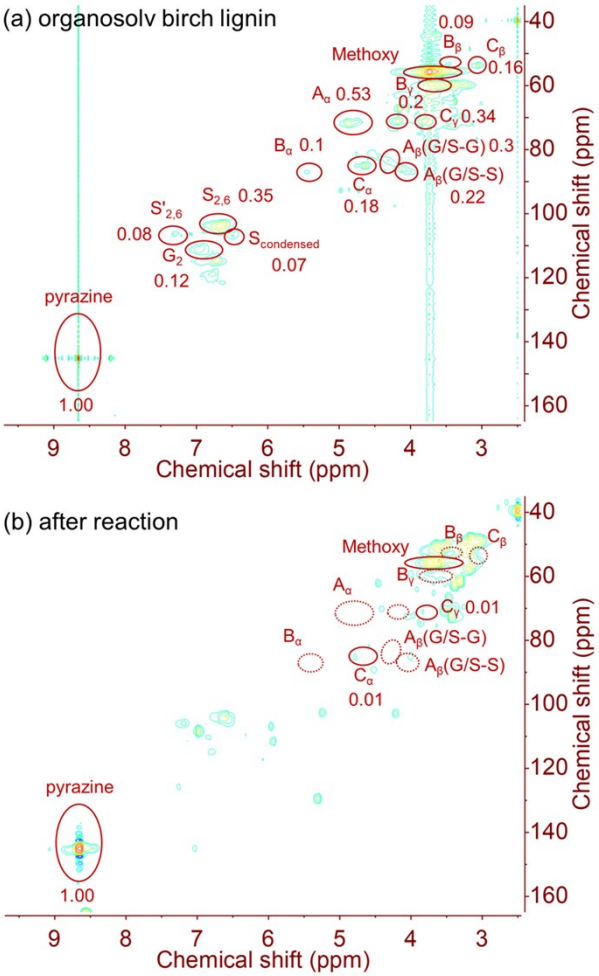

Figure S15. 2D HSQC NMR spectra (in DMSO-d_6) of (a) organosolv birch lignin and (b) catalytic cleavage reaction.

Before the 2D HSQC NMR test of dioxasolv birch lignin, to the DMSO-d_6 solution of dioxasolv birch lignin (50 mg), the pyrazine was added as an internal standard. And the H atoms' peak area of pyrazine is normalized as 1.00 according to the integral of ^{1}H NMR. Thus, the integral peak areas of β-O-4 linkage (A_α, A_β), β-5 linkage (B_α, B_β, B_γ), and β-β linkage (C_α, C_β, C_γ), to internal standard were calculated as (0.53, 0.52), (0.1, 0.09, 0.2), and (0.18, 0.16, 0.34), according to the integral of ^{1}H NMR of dioxasolv birch lignin. After oxidative depolymerization (dioxasolv birch lignin: 50 mg), the signals of β-O-4 linkage (A) and β-5 linkage (B) almost disappeared, suggesting that the β-O-4 linkage (A) and β-5 linkage (B) were completely converted. But the signal of the part of the β-β linkages (C) was still observed, and the peak areas of both C_α and C_γ to internal was calculated as 0.01. Thus, the conversions of C_α and C_γ in β-β linkages were calculated referred to internal:[3] 100*[1-0.01/[(0.18)*(50/50)]] = 94% and 100*[1-0.01/[(0.34)*(50/50)]] = 97%.

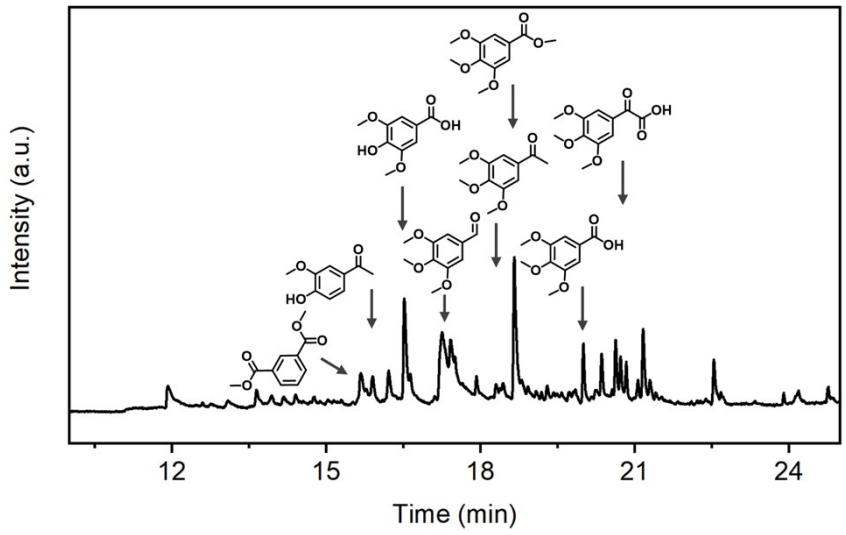

Figure S16. The distribution of aromatic monomeric products for dioxasolv birch lignin.

^{1}H NMR Spectra of Lignin β-O-4 Model Compounds

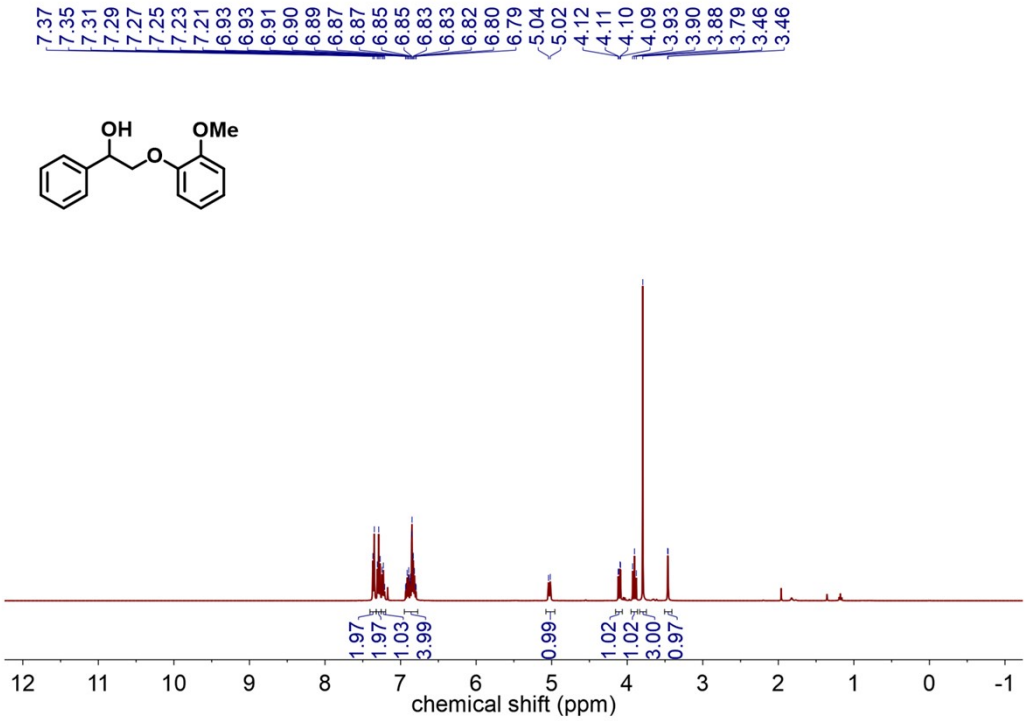

Figure S17. ^{1}H NMR of 2-(2-Methoxyphenoxy)-1-phenylethanol.

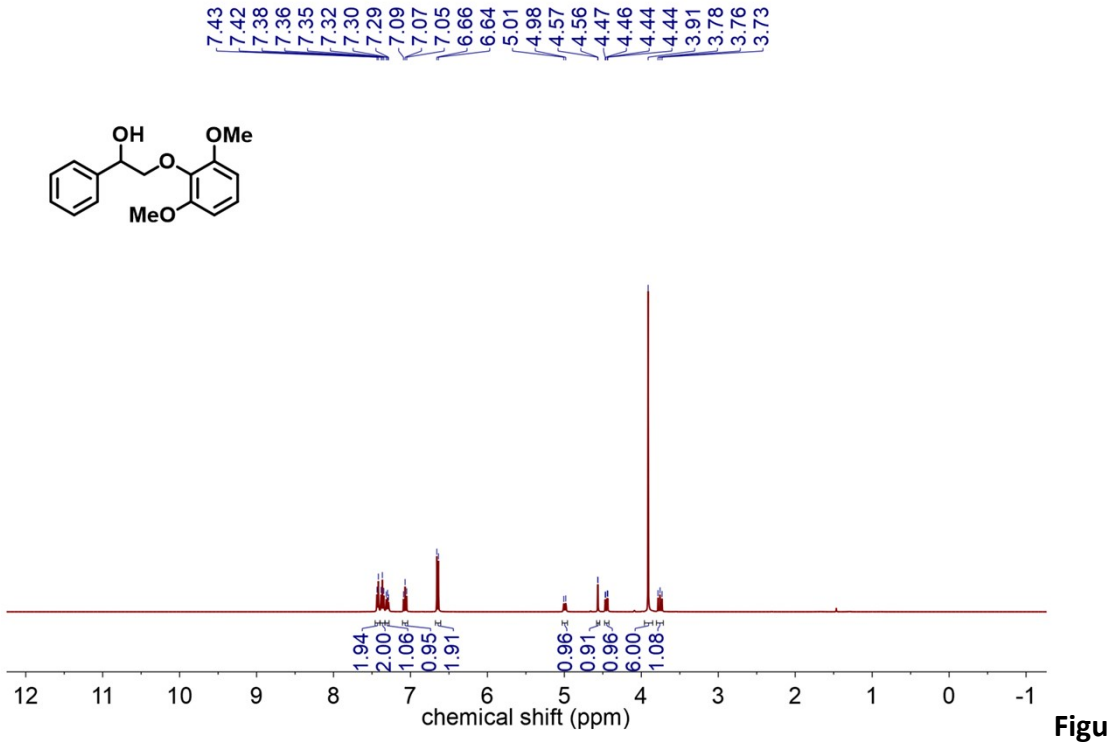

Figure S18. ^{1}H NMR of 2-(2,6-Dimethoxyphenoxy)-1-phenylethanol.

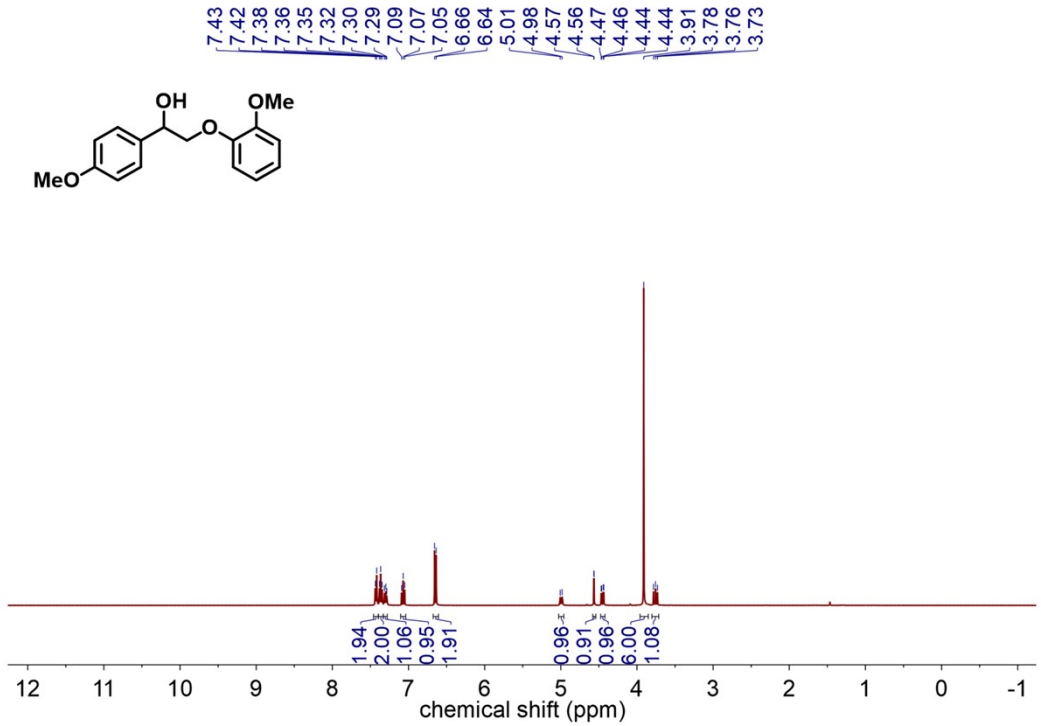

Figure S19. ^{1}H NMR of 2-(2-Methoxyphenoxy)-1-(4-methoxyphenyl)ethanol.

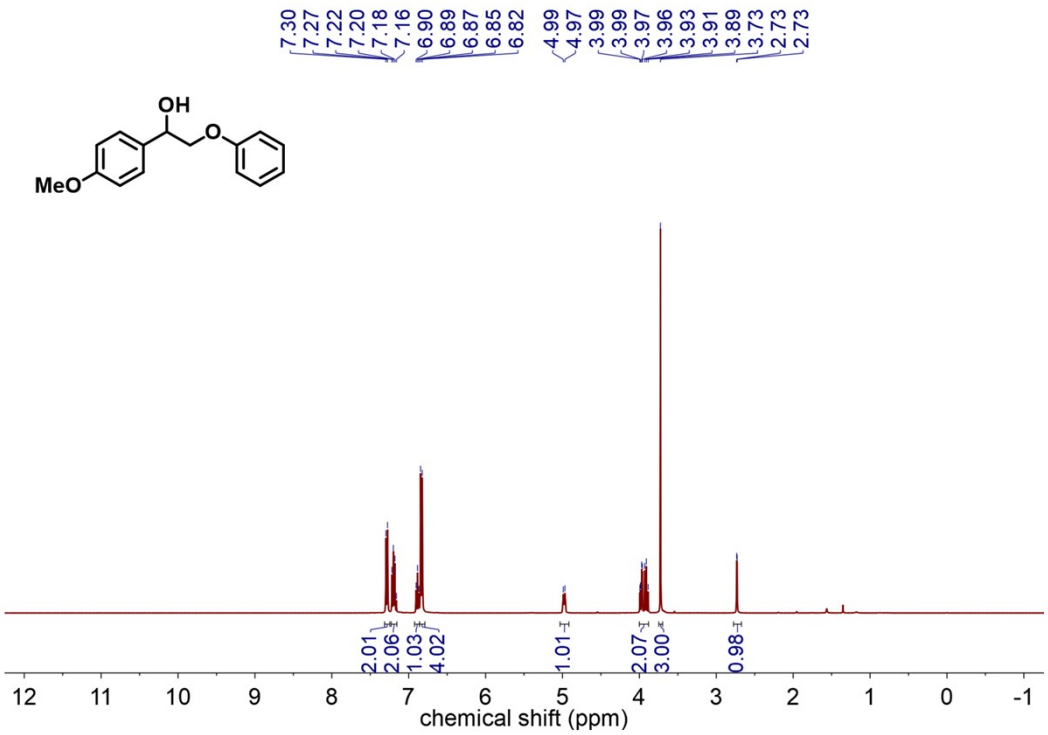

Figure S20. ^{1}H NMR of 1-(4-Methoxyphenyl)-2-phenoxyethanol.

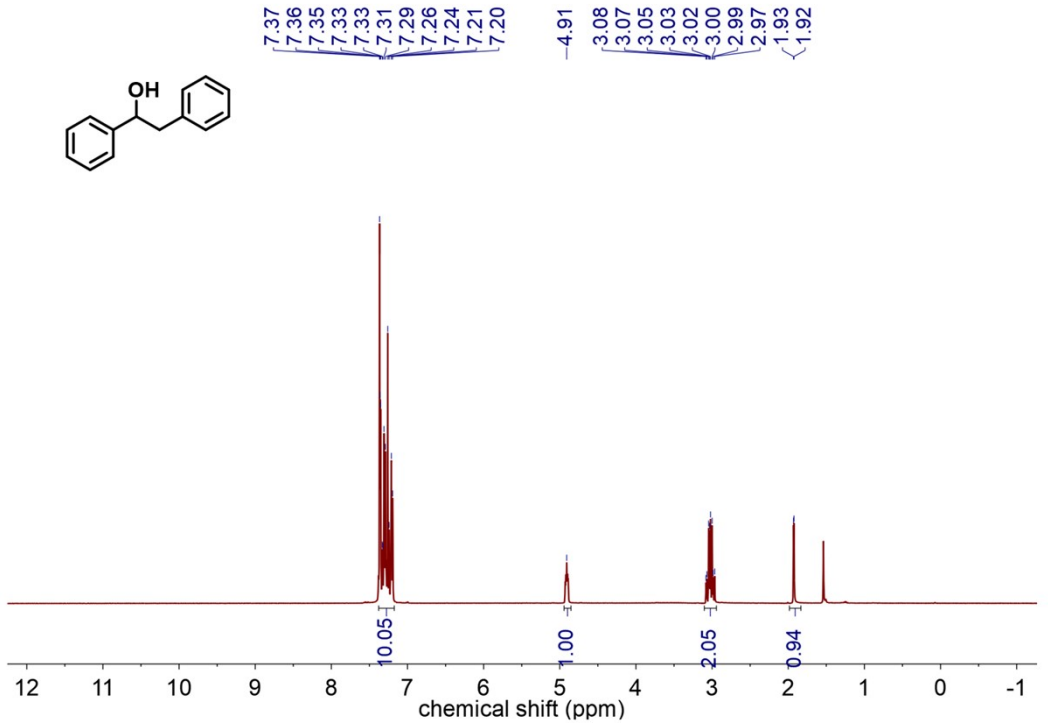

Figure S21. ^{1}H NMR of 1,2-diphenylethanol

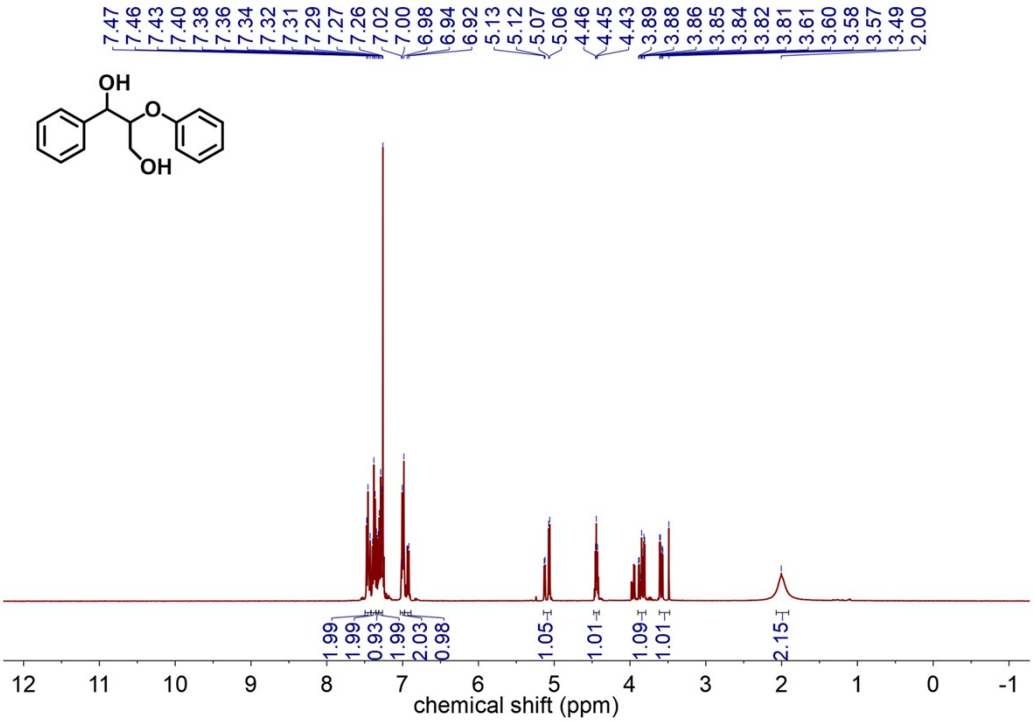

Figure S22. ^{1}H NMR of 2-phenoxy-1-phenylpropane-1,3-diol

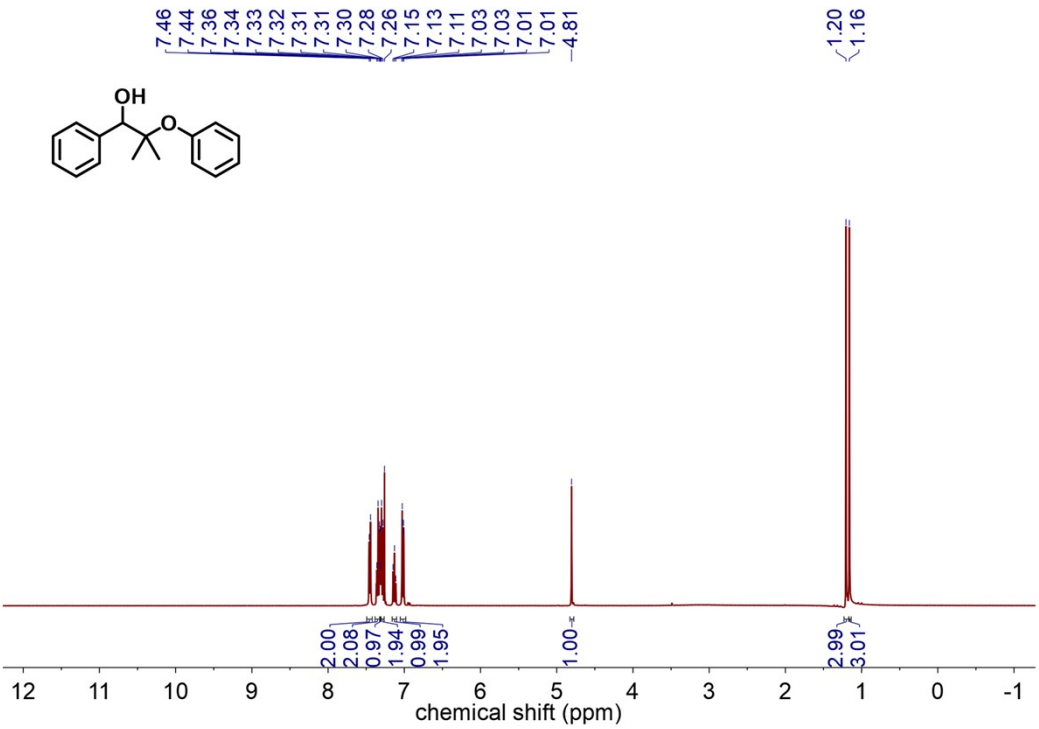

Figure S23. ^{1}H NMR of 2-methyl-2-phenoxy-1-phenylpropan-1-ol

References

[1] Zhao, L.; Shi, S.; Zhu, G.; Liu, M.; Gao, J.; Xu, J. Au–Pd alloy cooperates with covalent triazine frameworks for the catalytic oxidative cleavage of β-O-4 linkages. *Green Chem.* **2019,** *21*, 6707-

6716.
[2] Luo, H. H.; Wang, L. Y.; Li, G. S.; Shang, S. S.; Lv, Y.; Niu, J. Y.; Gao, S. Nitrogen-doped carbon-modified cobalt-nanoparticle-catalyzed oxidative cleavage of lignin β-O-4 model compounds under mild conditions. *ACS Sustain. Chem. Eng.* **2018,** *6*, 14188-14196.
[3] Zhu, G. Z.; Shi, S.; Zhao, L.; Liu, M.; Gao, J.; Xu, J. Catalytic activation of carbon–hydrogen bonds in lignin linkages over strong-base-modified covalent triazine frameworks for lignin oxidative cleavage. *ACS Catal.* **2020,** *10*, 7526-7534.
[4] Rahimi, A.; Azarpira, A.; Kim, H.; Ralph, J.; Stahl, S. S. Chemoselective Metal-Free Aerobic Alcohol Oxidation in Lignin. *J. Am. Chem. Soc.* **2013,** *135*, 6415-6418.
[5] Deng, W.; Zhang, H.; Wu, X.; Li, R.; Zhang, Q.; Wang, Y. Oxidative conversion of lignin and lignin model compounds catalyzed by CeO_2-supported Pd nanoparticles. *Green Chem.* **2015,** *17*, 5009-5018.
[6] Song, W. L.; Dong, Q. M.; Hong, L.; Tian, Z. Q.; Tang, L. N.; Hao, W. L.; Zhang, H. X. Activating molecular oxygen with Au/CeO_2 for the conversion of lignin model compounds and organosolv lignin. *RSC Advances* **2019,** *9*, 31070-31077.
[7] Lei, P.; Zhang, J.; Shen, W.; Zhong, M.; Guo, S. Boosting the catalytic performance of Ru nanoparticles in the cleavage of β-O-4 linkages in lignin by doping Mo. *Green Chem.* **2024,** *26*, 6616-6624.
[8] Liu, S.; Bai, L.; van Muyden, A. P.; Huang, Z.; Cui, X.; Fei, Z.; Li, X.; Hu, X.; Dyson, P. J. Oxidative cleavage of β-O-4 bonds in lignin model compounds with a single-atom Co catalyst. *Green Chem.* **2019,** *21*, 1974-1981.
[9] Sun, K.; Chen, S.; Zhang, J.; Lu, G. P.; Cai, C. Cobalt Nanoparticles Embedded in N-Doped Porous Carbon Derived from Bimetallic Zeolitic Imidazolate Frameworks for One-Pot Selective Oxidative Depolymerization of Lignin. *ChemCatChem* **2019,** *11*, 1264-1271.
[10] Wang, M.; Lu, J. M.; Zhang, X. C.; Li, L. H.; Li, H. J.; Luo, N. C.; Wang, F. Two-step, catalytic C–C bond oxidative cleavage process converts lignin models and extracts to aromatic acids. *ACS Catal.* **2016,** *6*, 6086-6090.
[11] Wang, Y.; Ding, B.; He, J.; Ding, Z.; Hou, Z. Ionic Liquid-Stabilizing Vanadium Oxo-Cluster Catalysts for One-Step Selective Oxidative Cleavage of β–O–4 Lignin Model Compounds. *Energy & Fuels* **2023,** *37*, 5429-5440.
[12] Hanson, S. K.; Baker, R. T.; Gordon, J. C.; Scott, B. L.; Thorn, D. L. Aerobic Oxidation of Lignin Models Using a Base Metal Vanadium Catalyst. *Inorg. Chem.* **2010,** *49*, 5611-5618.
[13] Tian, H. R.; Liu, Y. W.; Zhang, Z.; Liu, S. M.; Dang, T. Y.; Li, X. H.; Sun, X. W.; Lu, Y.; Liu, S. X. A multicentre synergistic polyoxometalate-based metal–organic framework for one-step selective oxidative cleavage of β-O-4 lignin model compounds. *Green Chem.* **2020,** *22*, 248-255.
[14] Li, Y.; Zhang, X.; Li, Z.; Song, J.; Wang, X. Full Utilization of Lignocellulose with Ionic Liquid Polyoxometalates in a One-Pot Three-Step Conversion. *ChemSusChem* **2019,** *12*, 4936-4945.
[15] Xin, X.; Li, Z.; Chi, M.; Zhang, M.; Dong, Y.; Lv, H.; Yang, G.-Y. A recoverable polyoxometalate-ionic liquid catalyst for selective cleavage of lignin β-O-4 models under mild conditions. *Green Chem.* **2023,** *25*, 2815-2824.
[16] Li, Z.; Li, Y.; Chen, Y.; Wang, Q.; Jadoon, M.; Yi, X.; Duan, X.; Wang, X. Developing Dawson-Type Polyoxometalates Used as Highly Efficient Catalysts for Lignocellulose Transformation. *ACS Catal.* **2022,** *12*, 9213-9225.
[17] Li, J.; Li, Z.; Dong, J.; Fang, R. B.; Chi, Y. N.; Hu, C. W. Hexaniobate as a Recyclable Solid Base

Catalyst to Activate C–H Bonds in Lignin Linkage Boosting the Production of Aromatic Monomers. *ACS Catal.* **2023,** *13*, 5272-5284.
[18] Zhao, L.; Shi, S.; Liu, M.; Zhu, G.; Wang, M.; Du, W.; Gao, J.; Xu, J. Covalent triazine framework catalytic oxidative cleavage of lignin models and organosolv lignin. *Green Chem.* **2018,** *20*, 1270-1279.
[19] Wang, M.; Li, L. H.; Lu, J. M.; Li, H. J.; Zhang, X. C.; Liu, H. F.; Luo, N. C.; Wang, F. Acid promoted C–C bond oxidative cleavage of β-O-4 and β-1 lignin models to esters over a copper catalyst. *Green Chem.* **2017,** *19*, 702-706.
[20] Hu, Y. Z.; Yan, L.; Zhao, X. L.; Wang, C. G.; Li, S.; Zhang, X. H.; Ma, L. L.; Zhang, Q. Mild selective oxidative cleavage of lignin C–C bonds over a copper catalyst in water. *Green Chem.* **2021,** *23*, 7030-7040.
[21] Li, L. X.; Kong, J. H.; Zhang, H. M.; Liu, S. J.; Zeng, Q.; Zhang, Y. Q.; Ma, H.; He, H. Y.; Long, J. X.; Li, X. H. Selective aerobic oxidative cleavage of lignin C-C bonds over novel hierarchical Ce-Cu/MFI nanosheets. *Appl. Catal. B: Environ.* **2020,** *279*, 119343-119358.
[22] Guo, S.; Tong, X.; Meng, L.; Yang, G. A sustainable iron-catalyzed aerobic oxidative C–C and C–O bond cleavage of a lignin model to phenol and methyl benzoate. *Catal. Sci. & Technol.* **2023,** *13*, 1748-1754.